JOURNAL OF AGRICULTURAL AND FOOD CHEMISTRY

Article

pubs.acs.org/JAFC

Biosorption of Heavy Metal Ions onto Agricultural Residues Buckwheat Hulls Functionalized with 1-Hydroxylethylidenediphosphonic Acid

Ping Yin,* Zengdi Wang, Rongjun Qu,* Xiguang Liu, Jiang Zhang, and Qiang Xu

School of Chemistry and Materials Science, Ludong University, Yantai 264025, P. R. China

Supporting Information

ABSTRACT: Novel biosorbent materials obtained from agricultural residues buckwheat hulls (BH) were successfully developed through functionalization with 1-hydroxylethylidenediphosphonic acid (HEDP), and they were characterized. This paper reports the feasibility of using HEDP-BH for removal of heavy metals from stimulated wastewater, the experimental results revealed that the adsorption property of functionalized buckwheat hulls with 120 mesh 120-HEDP-BH for Au(III) was very excellent, and the monolayer maximum adsorption capacity for Au(III) calculated from the Langmuir isotherm models was up to 450.45 mg/g at 35 °C. The combined effect of initial solution pH, 120-HEDP-BH dosage, and initial Au(III) concentration was investigated using response surface methodology (RSM), and the result showed that biomass dosage exerted a stronger influence on Au(III) uptake than those of initial pH and initial Au(III) concentration. Analysis of variance (ANOVA) of the quadratic model demonstrated that the model was highly significant. Moreover, investigation on the adsorption selectivity showed that 120-HEDP-BH displayed strong affinity for gold in aqueous solutions and even exhibited 100% selectivity for Au(III) ions in the presence of Zn(II) and Co(II). Regeneration capacities of 120-HEDP-BH were studied using the eluent solutions of 0.0−5.0% thiourea in 0.1 mmol/L HCl, and it was found that the adsorption capability remains high after several cycles of adsorption−desorption process.

KEYWORDS: *agricultural residues, buckwheat hulls, functionalization, 1-hydroxylethylidenediphosphonic acid, heavy metal removal*

INTRODUCTION

Heavy metal ions present in groundwater and surface water are a threat to human and local environment; they are not biodegradable and tend to accumulate in organisms causing various diseases and disorders.[1,2] Thus, removal and recovery of heavy metal ions from wastewater have been a significant concern for economic and environmental factors. In recent years, attention was focused on the methods for recovery and reuse of metals rather than disposal, and the adsorption process seems to be the most versatile and effective method if combined with appropriate regeneration steps.[3,4] Consequently, effective adsorbents with strong affinities and high loading amount for heavy metal ions were searched for.

Biosorption for removal of heavy metals from industrial wastewater, in regard with its simplicity, has gained important credibility in recent years, due to the good efficiency, minimization of secondary wastes, and low cost of these biomass-based materials. [5] Recently, abundant waste materials from agricultural activities may be low-cost adsorbents for heavy metal removal, and it can convert agricultural waste, of which billions of kilograms are produced annually, to useful, value-added adsorbents. Therefore, studies on these low-cost adsorbents that have metal-binding capacities have been intensified since adsorption technology, which is highly effective, simple, and economical, and the agricultural residues, such as spent-grain rice, barley husk, and rice husk, etc., which are locally available in large quantities, can be utilized as low-cost adsorbent materials.[6,7] Buckwheat is at present considered a food component of high nutritional value; it has become popular as a kind of healthy food, since it was reported that its seeds contain many biologically active compounds. As one kind of agricultural residual, buckwheat hull is rich in cellulose and has carboxyl and hydroxyl functional groups. Spent buckwheat hulls were chosen to be applied as an absorbent material due to its granular structure, insolubility in water, well-functionalized surface property, high mechanical strength, and local availability at almost no cost. However, many of the naturally available adsorbents have low metal removal and slow process kinetics. Thus, it is necessary to develop innovative inexpensive adsorbents with good affinity toward metal ions. Surface functionalization technology has been proven to be effective. Functional groups presenting in the biopolymer structure can provide binding sites to remove the metal ions from aqueous solutions and improve the adsorption properties. [8]

To date, no report is available on adsorption investigation of organophosphonic acid-functionalized spent buckwheat. In view of the above, the objective of this study was to investigate the feasibility of using 1-hydroxylethylidenediphosphonic acid-functionalized buckwheat hulls as biosorbent for heavy metals removal from aqueous media. Introduction of the organophosphonic acid groups onto agricultural residues buckwheat hulls can make the biomaterial form stable chelating compounds with transition metal ions. In the present work,

Received: August 16, 2012
Revised: October 29, 2012
Accepted: October 30, 2012
Published: October 30, 2012

dx.doi.org/10.1021/jf303565d | J. Agric. Food Chem. 2012, 60, 11664−11674

we explored the preparation of spent buckwheat hulls functionalized with 1-hydroxylethylidenediphosphonic acid with both the O donor atom in the hydroxyl group and the O donor atoms in the PO_3 group, which could make the material have excellent coordination properties with transition metal ions and obtain a novel adsorbent with high loading of metal ions and sorption selectivity for some particular metal ions. After its adsorption of Au(III), Hg(II), Cu(II), Co(II), Cd(II), Cr(III), Zn(II), and Ni(II) metal ions was studied, the results displayed that 120-HEDP-BH had an excellent adsorption amount for Au(III) metal ion. It is well known that precious metals are widely used in the fields of industry and medicine due to their specific physical and chemical properties. Because of the value and scarcity of precious metals such as gold, it is necessary to treat these waste aqueous solutions and try to recover them economically. Furthermore, the response surface methodology (RSM) has been employed to optimize the relevant adsorption process parameters, and it is also possible to observe the effects of individual variables and their combinations of interactions on the response using RSM.[9] Moreover, the adsorption selectivity and adsorption reproducibility of this functionalized buckwheat hulls 120-HEDP-BH for Au(III) ions from aqueous solutions were also investigated.

EXPERIMENTAL DETAILS

Materials and Methods. Spent buckwheat hulls were collected from a buckwheat production site (Yantai, China) and washed with deionized water, dried at 50 °C, and then ground in a mill to pass through 30, 60, 90, and 120 mesh sieves to obtain different uniform particle size for further processing. A 10.0 g amount of powdered biomass was agitated at 60 °C for 24 h in 50 mL of 20.0% 1-hydroxylethylidenediphosphonic acid (HEDP) solution for surface functionalization reaction. The resulting biomasses were filtered and dried; then, the treated sample was thermochemically reacted for 4 h by elevating oven temperature at 120 °C, and the mixture was allowed to enter reaction. Products obtained were mixed in deionized water for 30 min, filtered, and washed with deionized water. 1-Hydroxyethylidenediphosphonic acid-functionalized buckwheat hulls (HEDP-BH) were dried in the oven. Finally, the functionalized hulls were vacuum oven dried at 45 °C for 48 h. Thermally treated sample was cooled to room temperature and stored for the following adsorption experiments.

All other reagents utilized in the experiments were analytical grade and used without any further purification, and all solutions were prepared with deionized water. Stock solutions of containing various metal ions at a certain concentration were prepared by dissolving their relative metal salts (Sinopharm Chemical Reagent Co., Ltd., China) in deionized water. The pH of the solution containing Au(III) was adjusted with hydrochloric acid aqueous solution (1 mol/L) and sodium hydroxide aqueous (1 mol/L), while those of the solution containing other metal ions were adjusted with ammonium acetate/nitric acid solutions.

Infrared spectra (FT-IR) of samples were reported in the range of 4000−400 cm^{-1} with a resolution of 4 cm^{-1} by accumulating 32 scans using a Nicolet MAGNA-IR 550 (series II) spectrophotometer. KBr pellets were used for solid samples, and the Omnic32 software (Nicolet Inc., USA) and Origin8 software (OriginLab, Inc., USA) were used to collect spectra and develop the statistics, respectively. The morphology of the compounds was examined on a JEOL JSF5600LV scanning electron microscope (JEOL Co., Japan). EDXAS was performed on a NORAN LEVER-2 EDX analytical instrument. Before observation, the sample was placed on a specimen stub covered with a conductive adhesive tab and provided with a sputtered 15 nm platinum coating. Powder X-ray diffraction (XRD) data were obtained using a Rigaku Max-2500VPC diffractometer with Cu Kα_1 radiation (λ = 1.54056 Å). Thermogravimetric analysis (TG) was recorded on a Netzsch STA 409. Test conditions: type of crucible, DTA/TG crucible Al_2O_3; nitrogen atmosphere, flow rate 30 mL/min; heating rate, 10 K/min. Atomic absorption analysis of transition metal ions was performed with a flame atomic absorption spectrophotometer (GBC-932A, made in Australia), and the SpectrAA software (Varian Australia Pty.Ltd.) and Origin8 software (OriginLab.Inc.USA) were were used to collect spectra and develop the statistics, respectively.

Computational Details. Density functional theory calculations of 1-hydroxylethylidenediphosphonic acid have been performed with the Gaussian 03 program using the B3LYP/6-31G(d) basis set to obtain the optimized molecular structure and vibrational wavenumbers. Frequencies for the required structure were evaluated at the B3LYP/6-31G(d) level to ascertain the nature of stationary points, and harmonic vibrational wavenumbers were calculated using the analytic second derivatives to confirm the convergence to the minimum of the potential surface. Moreover, the Mulliken atomic charges were also obtained at the B3LYP/6-31G(d) level.

Saturation Adsorption Experiments for Transition Metal Ions. The saturation adsorption experiment was employed to determine the adsorption amounts of HEDP-BH with different meshes for different kinds of metal ions, and they were carried out with shaking 30.0 mg of the adsorbent with 10.0 mL of metal ion solution (2.0 mmol/L). The mixture was equilibrated for 24 h on a thermostat-cum-shaking assembly at 25 °C. Each batch of experiment was carried out in triplicate, and the mean values showed a maximum standard deviation of ±5%. The adsorption amount was calculated according to eq 1

$$q = \frac{(C_o - C_e)V}{W} \tag{1}$$

where q is the adsorption amount (mmol/g), C_o and C_e are the initial and equilibrium concentrations of metal ions (mmol/mL) in solution, respectively, V is the volume of the solution (mL), and W is the weight of HEDP-BH(g).

Adsorption Isotherms. The isotherm adsorption property of the adsorbents was investigated also by batch tests. In a typical procedure, a series of 20 mL tubes was used. Adsorption isotherms were studied using 20.0 g of the adsorbent with 10.0 mL of various Au(III) ion concentrations at 25 °C and pH = 2.5 for 24 h. Modeling of the adsorption isotherm data was conducted by the linear fitting using the Origin8 software program (OriginLab, Inc., USA).

Response Surface Methodology (RSM). The effects of three independent variables, initial pH, adsorbent dosage, and initial Au(III) concentration, were investigated by means of central composite design (CCD). Experimental design was carried out by three chosen independent process variables at three levels. For each factor, the experimental range and central point were shown in Table 1. The

Table 1. Coded Levels for Independent Factors Used in the Experimental Design

factors	symbol	coded levels		
		−1	0	+1
initial pH	X_1	2.0	2.5	3.0
adsorbent dosage/mg	X_2	10	20	30
initial Au(III) concentrations/mmol/L	X_3	6.070	7.284	8.498

software of Minitab was used for designing and analyzing the experimental data. Independent variables (factors) and their levels, real values as well as coded values, are presented in Table 1.

The model equation was used to predict the optimum value and subsequently elucidate the interaction between the factors. The quadratic equation model for predicting the optimal point was expressed according to eq 2

$$Y = \lambda_0 + \sum_{i=1}^{4} \lambda_i x_i + \sum_{i=1}^{4} \lambda_{ii} x_i^2 + \sum_{i=1}^{3} \sum_{j=i+1}^{4} \lambda_{ij} x_i x_j \tag{2}$$

where λ_0, λ_i, λ_{ii}, and λ_{ij} are regression coefficients (λ_0 is a constant term, λ_i is the linear effect term, λ_{ii} is the squared effect term, and λ_{ij} is the interaction effect term) and Y is the predicted response value. All data were analyzed with the assistance of the software of Minitab, and significant second-order coefficients were selected by regression analysis with backward elimination. Then, the fit of the model was evaluated by coefficients of determination and a test for lack of fit, which was performed by comparing mean square lack of fit to mean square experimental error, from analysis of variance (ANOVA).

Competitive Adsorption. In order to investigate the adsorption selectivity of the adsorbent for Au(III), 20.0 mg of adsorbents was added into 10 mL solutions (binary system containing equal initial concentrations (2.0 mmol/L) of Au(III) ion and other coexisting metal ions), and the mixture was shaken for 24 h. The initial pH was adjusted to 2.5 with the temperature at 25 °C.

Desorption and Recycling Studies. To investigate the desorption ability of the adsorbed Au(III) ions form the adsorbent, desorption experiments were carried out as follows: After adsorption, the Au(III) ion-loaded adsorbents were separated and slightly washed with deionized water to remove unadsorbed Au(III) ions on the surface of the adsorbent. They were then stirred in the different solutions of 0.1 mmol/L HCl, 0.1 mmol/L HCl + 1.0% thiourea, 0.1 mmol/L HCl + 2.0% thiourea, 0.1 mmol/L HCl + 3.0% thiourea, 0.1 mmol/L HCl + 4.0% thiourea, and 0.1 mmol/L HCl + 5.0% thiourea, which were employed as the desorption medium, at 25 °C for 24 h. The desorption ratio of Au(III) ions was then calculated as the ratio of the amount of desorbed Au(III) ions to the amount of initially absorbed Au(III) ions.

RESULTS AND DISCUSSION

Theoretical Calculations of the Modified Organic Group 1-Hydroxylethylidenediphosphonic Acid. The diphosphonic acids have proved to be good candidates for synthesis of open-framework or porous coordination polymer, in which the organic parts play a controllable spacer role and the two $-PO_3$ groups could chelate with metal ions to form one-, two-, or three-dimensional structures. [10] In the present work, HEDP was selected as the modified organic group to functionalize spent buckwheat hulls. Besides two $-PO_3$ groups, there is a $-OH$ group, which can also chelate with metal ions. Introduction of the organic groups onto buckwheat hulls can make the agricultural residues form stable chelating compounds with many heavy metal ions. In addition, phosphonic acid groups can provide several oxygen atoms to coordinate metal ions, which can be utilized to remove heavy metals from bleaching solution in the paper, pulp, and textile industry. [11] The aim of chemical functionalization with HEDP, which has both an O donor atom in the hydroxyl functional group and O donor atoms in the $-PO_3$ group, is to make the material have excellent coordination properties with metal ions and obtain a novel biosorbent with a high loading capacity and good adsorption selectivity for metal ions.

In order to design the title bioabsorbent material, we theoretically calculated the modified organic group at the B3LYP/6-31G(d) level in advance. In Scheme 1, the optimized structure of the modified organic group was displayed. The corresponding bond lengths, bond angles, and Mulliken atomic charges are presented in Tables S1 and S2 (Supporting Information). The absence of imaginary wavenumber on its calculated vibrational spectrum confirms that the structure deduced corresponds to minimum energy. P1−O6 and P12−O17 bond lengths are 1.4750 and 1.4820 Å, respectively, which agrees well with those values of phosphonic acid in ref 12 and a bit longer than the experimental value (1.47 Å). Moreover, P1−O2, P1−O4, P12−O13, and P12−O15 bond lengths are in the range 1.6098−1.6401 Å, comparable to those in phosphonic acid 1.59−1.63 Å. [12] Moreover, the bond angles A(7, 1, 2/4/6) and A(7, 12, 13/15/17)) are produced with reasonable accuracy as well. Table S2, Supporting Information, presents the Mulliken atomic charges of the ligand and shows that the oxygen atoms and nitrogen atom in phosphonic acid groups have more negative charges, and the Mulliken electronic populations of O2, O4, O6, O13, O15, O17, and O18, were −0.689, −0.673, −0.500, −0.700, −0.661, −0.554, and −0.655, respectively, which made these oxygen atoms chelate with metal ions more easily.

Scheme 1. Optimized Geometry of the Modified Group 1-Hydroxylethylidenediphosphonic Acid

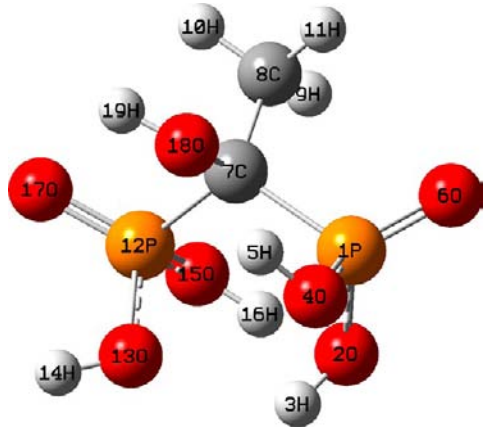

Saturation Adsorption of BH and HEDP-BH with Different Meshes. Figure 1 showed the saturation adsorption amounts of BH and HEDP-BH for transition metal ions, such Au(III), Hg(II),Cu(II), Pb(II), Co(II), Zn(II), Ni(II), and Cr(III) etc. As seen from Figure 1a, the particle size has an obvious influence on the adsorption capacity for heavy metal ions. In general, the smaller BH is, the higher the adsorption capacity is. For example, the adsorption capacity of BH with 30, 60, 90, and 120 mesh for Au(III) is 0.780, 0.681, 0.843, and 1.14 mmol/g, respectively. The research results displayed the static adsorption amounts of BH with 120 mesh for Au(III), Hg(II), and Cu(II) were 1.14, 0.806, and 0.262 mmol/g, respectively. However, those for Pb(II), Ni(II), Cd(II), Cr(III), Co(II), and Zn(II) metal ions were 0.157, 0.146, 0.148, 0.105, 0.0154, and 0.0708 mmol/g, respectively. BH had a good adsorption amount for Au(III), Hg(II), and Cu(II) metal ions, especially for Au(III) ion. Therefore, the buchwheat hulls with 120 mesh were selected for the subsequent functionalization process. Organophosphonic acid functional groups presenting in the BH biopolymer structure can further provide binding sites to remove the metal ions from aqueous solutions and improve the relevant adsorption properties. The adsorption capacity of 120-BH and 120-HEDP-BH was 1.14 and 1.81 mmol/g, respectively. It is obvious in Figure 1b that 120-HEDP-BH has a higher adsorption property than 120-BH, and the results showed that surface modification markedly improved the adsorption capacity. Through organophosphonic acid groups, 120-HEDP-BH can form the stable chelating compounds with many transition metal ions, especially with Au(III). Moreover, it was clear that the adsorption capacity of 120-HEDP-BH was relatively high when compared to several other adsorbents such as modified silica gel with hydroxyl- or amino-terminated polyamine, thiol cotton fiber, Alfalfa biomass, and poly(vinylbenzylchloride-acrylonitryle-divinylbenzene)

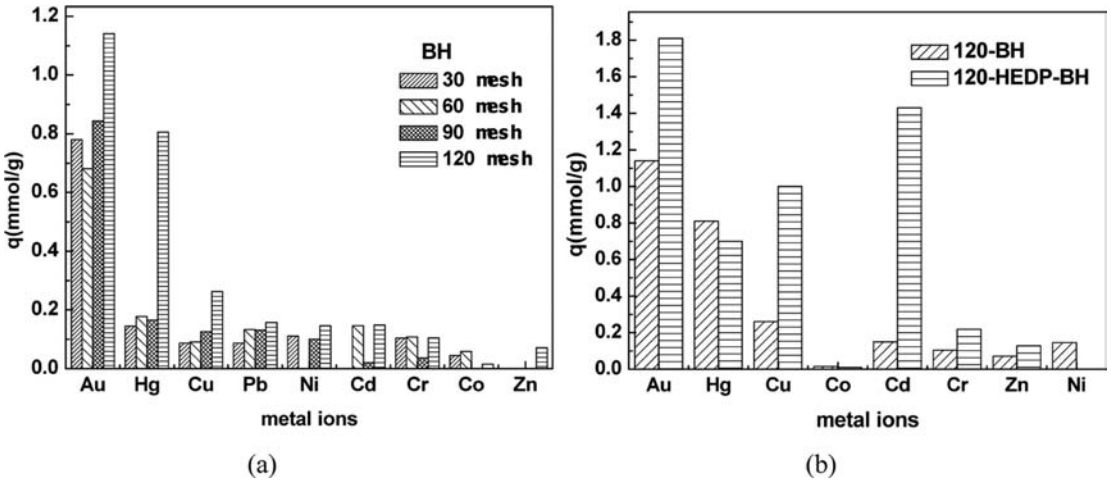

Figure 1. Static adsorption capacities of BH (particle size 30, 60, 90, and 120 mesh) and 120-HEDP-BH (particle size 120 mesh) for heavy metal ions at room temperature.

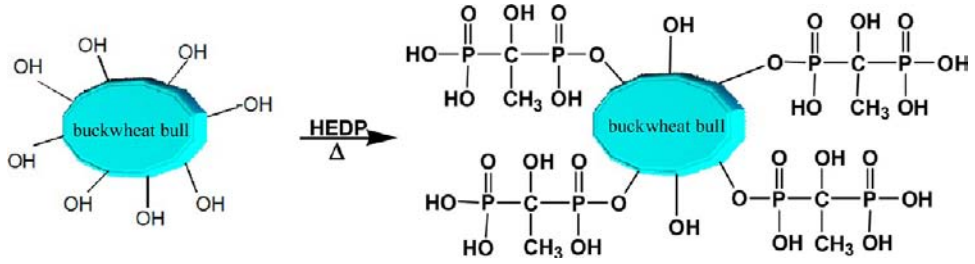

Figure 2. Preparation of the adsorbent HEDP-BH obtained form agricultural residues by thermochemical reaction.

modified with amino and guanidine ligands.[13−16] According to the theory of hard and soft acids and bases (HSAB) defined by Pearson, metal ions will have a preference for coordinating with ligands that have more or less electronegative donor atoms. Oxygen is a hard base while gold is a soft acid according to HSAB; therefore, only a few studies on the interaction between these two elements have been reported. For example, Chen et al. synthesized gold(III) tetraarylporphyrin phosphonate derivatives.[17] Kojima et al. synthesized gold complexes bearing phosphoric acids used in asymmetric catalysis.[18] Gardea-Torresdey and Yin et al. found that the carboxyl group/phosphonic acid group plays some role in the binding of Au(III) and higher gold(III) binding at low pHs.[19,20] Moreover, gold is one of the precious metals widely used in various areas, and it is a toxic element, causing allergic eczematous dermatitis and some nephrotoxic effects on humans. Because of its increasing presence in the environment, growing interest is in the elucidation of its role in living organisms and impact on human health.[21] Zammit et al. reviewed the development of novel biotechnologies and the role they would play in gold process and remediation.[22] Navarro et al. reported a more environmentally friendly process for gold, and they utilized the adsorption technology with activated carbon to separate the gold ions from solution.[23] The above-mentioned research shows that the low-cost 120-HEDP-BH is favorable and useful for removal of precious metal ions, and the high adsorption capacity makes it a promising candidate material for Au(III) uptake. Therefore, in the following, the adsorption behavior of the adsorbent 120-HEDP-BH for Au(III) was investigated particularly. In order to investigate the effect of the initial pH on the gold ions adsorption behavior, adsorption experiments were conducted in the pH range of 1.0−4.0, and the effect of pH on the adsorption for Au(III) on 120-HEDP-BH is illustrated in Figure S1 (Supporting Information). The results showed that the good adsorption capacities of the adsorbent for Au(III) were at about pH 2.5. Consequently, all of the following experiments were performed at pH 2.5. Before the adsorption investigation, it is necessary to carry out characterization of the adsorbent 120-HEDP-BH, since there is a close relation between the microstructure and the adsorption property of the relevant adsorbent material.

Characterization of the Adsorbent 120-BH and 120-HEDP-BH. HEDP-BH has been developed as described in the Experimental Details, the thermochemical reaction of HEDP-BH is shown in Figure 2, and the FTIR spectra of 120-BH and 120-HEDP-BH are displayed in Figure 3. When the organophosphonic acid HEDP is heated, it will dehydrate to yield a reactive anhydride. Then BH is present in the reaction mixture; the anhydride can react with BH to form a BH−phosphate adduct. Further heating can result in additional dehydration with the possibility of cross-linking (Figure 2). The HEDP-BH adducts provided additional phosphonic acid groups when compared with untreated BH. To decide whether HEDP carried out the esterification reaction with BH, IR spectroscopic analysis of both 120-BH and 120-HEDP-BH was investigated. As seen from Figure 3, the broad peak at about 3400 cm^{-1} was the characteristic peak of BH corresponding to the presence of hydroxyl groups of cellulose. The strong C−O−C band at around 1036 cm^{-1} also confirmed the cellulose structure, while in the IR spectrum of 120-HEDP-BH there are two major changes could be observed by comparing it with that of 120-BH: one is the appearance of both P═O at 1174 cm^{-1} and the

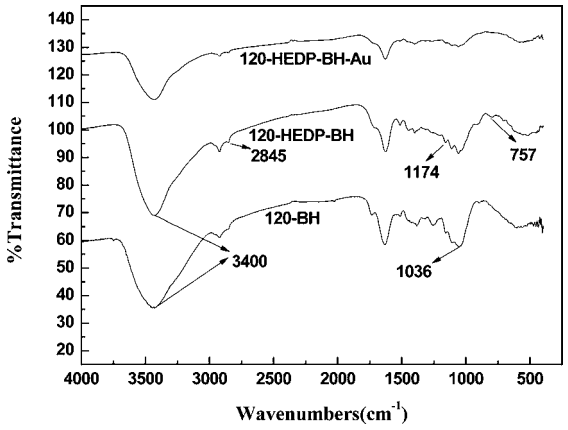

Figure 3. FT-IR spectra of 120-BH, 120-HEDP-BH, and 120-HEDP-BH-Au.

(C)−P−O stretching vibration peak at 757 cm^{-1}, and the other is a reduction in the hydroxyl (O−H) stretching band at around 3400 cm^{-1}. These facts reflected the result of organophosphonic acid esterification. Because of high amounts of introduced free phosphonic acid groups, it could be expected that organophosphonic acid-functionalized buckwheat hulls 120-HEDP-BH could have adequate chemical and physical characteristics to adsorb heavy metal ions.

Figure 4 shows SEM photographs of 120-BH and 120-HEDP-BH at 1000 times magnification. The sample morphologies of 120-BH and 120-HEDP-BH were characterized by SEM shown in Figure 4. Apparently, the surface of 120-BH became more rough after modification reactions, and more cavities on the surface of 120-HEDP-BH might increase the contact area and facilitate diffusion during adsorption, [24] and, consequently, improve its adsorption ability for heavy metal ions from aqueous media. It could be seen that the particle appearances of these samples were similar, demonstrating that the particles of 120-HEDP-BH had good mechanical stability, and they had not been destroyed during the whole reaction. Table 2 displayed the results of EDXAS spectrum for 120-BH and 120-HEDP-BH. It is obvious that there are peaks of C, O, Mg, P, K, and Ca. In particular, the weight percent of P in 120-HEDP-BH was 4.44%, which was higher that that in 120-BH (1.20%) after the thermochemical reaction of 120-BH and HEDP.

Figure 5a shows that all diffraction peaks of 120-BH and 120-HEDP-BH and their XRD patterns indicated the amorphous nature of the material lacking any crystallinity. This result showed that no essential change occurred in the topological structure of BH before and after the functionalized reactions, which implied that BH was stable enough to experience the chemical modification reactions. No novel diffraction peak appeared after the thermochemical reactions meant that the highly branched polymers on the surface of BH existed in a form of noncrystalline state. The TG curve could reflect the thermal stability of the material, and the thermal stability of 120-BH and 120-HEDP-BH has been determined by thermal analysis, and the results are shown in Figure 5b. Thermal analysis represents several steps of decomposition in the temperature range of 25−800 °C. The weight loss 8.3% and 10.3% in the temperature range of 25−200 °C corresponds to release of physically adsorbed water for 120-BH and 120-HEDP-BH, respectively. Further weight losses above 200 °C (64.8% and 44.7% for 120-BH and 120-HEDP-BH, respectively) are due to decomposition of the organic functional groups. It is noted that there is almost no weight loss for 120-HEDP-BH at 25−50 °C, and the adsorbents usually are utilized below 50 °C. Therefore, these data indicate that the resulting product 120-HEDP-BH has good thermal stability, and it should be applied at temperatures below 50 °C.

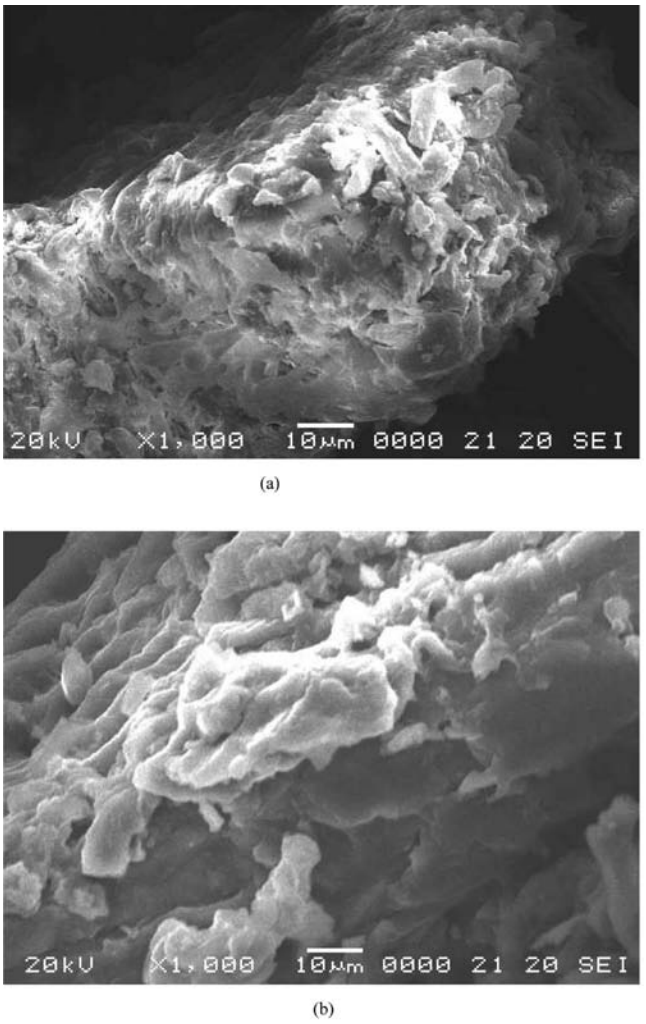

Figure 4. SEM images of 120-BH (a) and 120-HEDP-BH (b) at ×1000 magnification.

Adsorption Isotherms of 120-HEDP-BH for Au(III) Ions. Adsorption isotherms are very useful for finding out the adsorption capacity of the adsorbent, the solute−solute interaction, and the degree of accumulation of adsorbate on the surface of the adsorbent. Adsorption isotherms studied the relationship between the equilibrium adsorption capacity and the equilibrium concentration at a certain temperature, the adsorption isotherm of 120-HEDP-BH for Au(III) at 15, 25, and 35 °C was studied, and the results are shown in Figure 6. As seen in the figure, the absorption capacity of 120-HEDP-BH for Au(III) increased with the increase of the equilibrium concentration. The Langmuir and Freundlich isotherms are the most commonly used isotherms for different adsorbent/adsorbate systems to explain solid−liquid adsorption systems and predict their equilibrium parameters.[25] The Langmuir model assumes that the uptake of metal ions occurs on a homogeneous surface by monolayer adsorption without any interaction between adsorbed ions. The Freundlich model

Table 2. Results of Energy Spectrum Analysis of 120-BH and 120-HEDP-BH

absorbent	element	X-ray	int	error	*K*	*K* ratio	wt %	*A*%
120-BH	C	Ka	243.6	2.2072	0.7218	0.2641	52.89	60.65
	O	Ka	136.7	1.6534	0.2192	0.0802	44.19	38.05
	Mg	Ka	17.4	0.5899	0.0109	0.0040	0.77	0.44
	P	Ka	37.3	0.8638	0.0256	0.0094	1.20	0.53
	K	Ka	12.6	0.5021	0.0121	0.0044	0.52	0.18
	Ca	Ka	10.0	0.4467	0.0104	0.0038	0.44	0.15
120-BH total					1.0000	0.3659	100.00	100.00
120-HEDP-BH	C	Ka	116.0	1.5235	0.6413	0.2075	52.89	61.31
	O	Ka	75.8	1.2315	0.2268	0.0734	41.61	36.21
	Mg	Ka	6.5	0.3610	0.0076	0.0025	0.47	0.27
	P	Ka	84.9	1.3027	0.1086	0.0351	4.44	2.00
	K	Ka	5.8	0.3419	0.0104	0.0034	0.40	0.14
	Ca	Ka	2.7	0.2318	0.0052	0.0017	0.19	0.07
120-HEDP-BH total					1.0000	0.3235	100.00	100.00

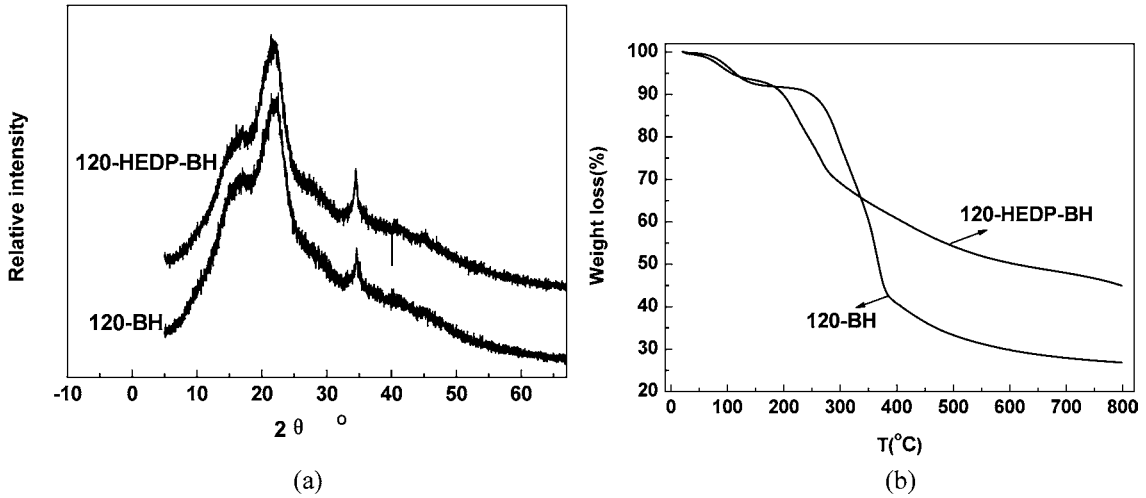

Figure 5. XRD patterns (a) and TG curves (b) of 120-BH and 120-HEDP-BH.

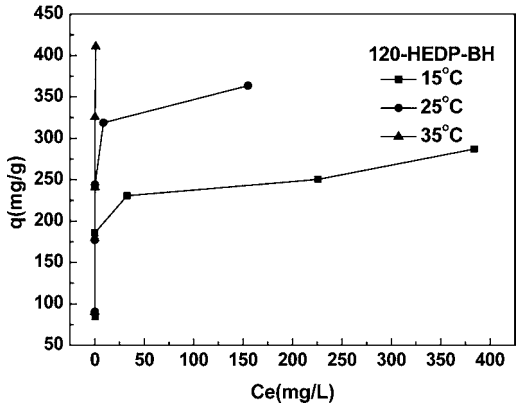

Figure 6. Adsorption isotherms of Au(III) onto 120-HEDP-BH at different temperatures.

assumes that the uptake or adsorption of metal ions occurs on a heterogeneous surface by monolayer adsorption. In order to understand the adsorption behavior, Langmuir eq 3 and Freundlich eq 4 were employed to fit the experimental data, respectively

$$\frac{C_e}{q_e} = \frac{C_e}{q} + \frac{1}{qK_L} \quad (3)$$

$$\ln q_e = \ln K_F + \frac{\ln C_e}{n} \quad (4)$$

where q_e is the adsorption capacity, mg/g, C_e is the equilibrium concentration of Au(III), mg/L, q is the saturated adsorption capacity, mg/g, K_L is the Langmuir constant, L/mg, n is the Freundlich constant, and K_F is the binding energy constant reflecting the affinity of the adsorbents to metal ions, mg/g. The R^2 value obtained from the Langmuir model is much closer to 1 than that obtained from the Freundlich model, suggesting the Langmuir model is better than the Freundlich model to fit the adsorption isotherm of 120-HEDP-BH for Au(III). The best-fit experimental equilibrium data in the Langmuir isotherm suggested monolayer coverage and chemisorption of Au(III) onto 120-HEDP-BH, and the maximum adsorption capacity of 120-HEDP-BH obtained by the Langmuir isotherm for Au(III) adsorption was 450.45 mg/g at 35 °C. It is clear that the adsorption capacity of 120-HEDP-BH was relatively high, due to the fact that 120-HEDP-BH has surface functional groups such as phosphonic acid groups that possess high affinity for gold ions. As we compared the adsorption capacity of different types of adsorbents used for Au(III) adsorption (Table S3, Supporting Information), it was clear that the adsorption capacity of 120-HEDP-BH was relatively high when compared to several other adsorbents such as silica gel chemically modified with hydroxyl- or amino-terminated polyamine, thiol

Table 3. Langmuir and Freundlich Isotherm Parameters for Au(III) Adsorption onto 120-HEDP-BH

		Langmuir			Freundlich		
adsorbent	T (°C)	q (mg/g)	K_L (L/mg)	R^2	K_F (mg/g)	n	R^2
120-HEDP-BH	15	280.90	0.1810	0.9938	156.37	10.3445	0.6341
	25	363.64	2.6442	0.9999	215.13	7.8958	0.6272
	35	450.45	10.3984	0.9847	448.20	2.9991	0.9713

cotton fiber, Alfalfa biomass, and poly(vinylbenzylchloride-acrylonitryle-divinylbenzene) modified with tris(2-aminoethyl)-amine, Table 3.[13−16] The above-mentioned research results show that the low-cost biomass-based 120-HEDP-BH is favorable and useful for removal of precious metal ions, and the high adsorption capacity makes it a promising candidate material for Au(III) uptake.

Response Surface Methodology. A prior understanding of the adsorption process and the process variable under investigation is necessary for achieving a more realistic model. The goal of our study was to model the adsorption capacity when 120-HEDP-BH was utilized as the adsorbent for Au(III) adsorption from stimulated wastewater. In order to improve the adsorption capacities and the efficiency of the work, the response surface methodology (RSM) is presented to indicate the parameters for an optimized adsorption process. It allows the user to gather large amounts of information from a small number of experiments and also observe the effects of individual variables and their combinations of interactions on the response.[26] RSM was applied to model the adsorption capacity of Au(III) from aqueous solutions with three reaction parameters: initial pH, adsorbent dosage, and initial Au(III) concentration. In the present study, CCD for the three variables was used as the experimental design model and RSM enabled us to obtain sufficient information for statistically acceptable results using a reduced number of experimental sets. The observed and predicted results of batch runs conducted in CCD-designed experiments are tabulated in Table 4. All of the 15 designed experiments were performed, and the levels ranged from 2.04 mmol/g to as high as 3.47 mmol/g. Application of the response surface methodology expressed in the following regression, eq 5, is an empirical relationship between the adsorption capacity (Y) and the tested variables taken in coded unit

$$Y = 2.28 - 0.02X_1 - 0.46X_2 - 0.13X_1^2 + 0.37X_2^2 + 0.24X_3^2 - 0.06X_1X_2 - 0.14X_1X_3 + 0.06X_2X_3 \quad (5)$$

where Y is the response, i.e., adsorption capacity, and X_1, X_2, and X_3 are the coded values of the main effects of initial pH, adsorbent dosage, and initial Au(III) concentration, respectively. The results of the coefficients of the model and analysis of variance (ANOVA) are shown in Table 5. The significance of each coefficient was determined by t and P values. The larger the magnitude of the it value and smaller the P value, the more significant is the corresponding coefficient. [27] Therefore, the variable with the largest effect was adsorbent dosage ($P < 0.001$). Moreover, the interaction of initial pH and initial Au(III) concentration (X_1X_3) wwas highly significant ($P = 0.009$), and the quadratic terms of adsorbent dosage (X_2^2) was very insignificant ($P < 0.001$). ANOVA indicated that the F_{model} value (63.93) with a low probability value ($P < 0.001$) demonstrates a high significance for the regression model. The goodness of the fit of the model was also checked by the multiple correlation coefficient (R^2). The value of the determination coefficient (R^2) was 0.9914, which indicated that the model was suitable to represent the real relationships among the selected reaction parameters. In this case, the value of the determination coefficient indicated that the sample

Table 4. Experimental Design and Results of the Response Surface Design

				adsorption capacities/mmol/g	
no.	X_1	X_2	X_3	experimental	fitted value
1	−1	0	1	2.54802	2.54200
2	0	0	0	2.28308	2.28306
3	1	0	1	2.22533	2.23211
4	1	−1	0	2.98576	3.03193
5	0	0	0	2.28306	2.28306
6	−1	−1	0	2.88252	2.94149
7	−1	0	−1	2.29207	2.28530
8	0	−1	1	3.34335	3.29041
9	0	1	1	2.43034	2.48253
10	1	1	0	2.04555	1.98659
11	1	0	−1	2.51719	2.52321
12	−1	1	0	2.19520	2.14903
13	0	0	0	2.28303	2.28306
14	0	−1	−1	3.47081	3.41862
15	0	1	−1	2.33576	2.38871

Table 5. Coefficients of the Model and ANOVA[a]

terms	coefficients	standard error	t start	P value
intercept	2.28306	0.03867	59.034	<0.001
X_1	−0.01800	0.02368	−0.760	0.482
X_2	−0.45945	0.02368	−19.400	<0.001
−3	−0.00860	0.02368	−0.363	0.731
X_1X_1	−0.12760	0.03486	−3.660	0.015
X_2X_2	0.37181	0.03486	10.666	<0.001
X_3X_3	0.24020	0.03486	6.891	0.001
X_1X_2	−0.06322	0.03349	−1.888	0.118
X_1X_3	−0.13695	0.03349	−4.089	0.009
X_2X_3	0.05551	0.03349	1.657	0.158

ANOVA

source	degrees of freedom	sum of squares	mean sum of squares	F	P
regression	9	2.58158	0.286842	63.93	<0.001
linear	3	1.69194	0.563979	125.69	<0.001
square	3	0.78631	0.262103	58.41	<0.001
interaction	3	0.10333	0.034445	7.68	0.026
residual error	5	0.02243	0.004487		
lack of fit	3	0.02243	0.007478		
pure error	2	0.00000	0.000000		
total	14	2.60402			

[a]Coefficient of determination (R^2) = 0.9914.

dx.doi.org/10.1021/jf303565d | J. Agric. Food Chem. 2012, 60, 11664−11674

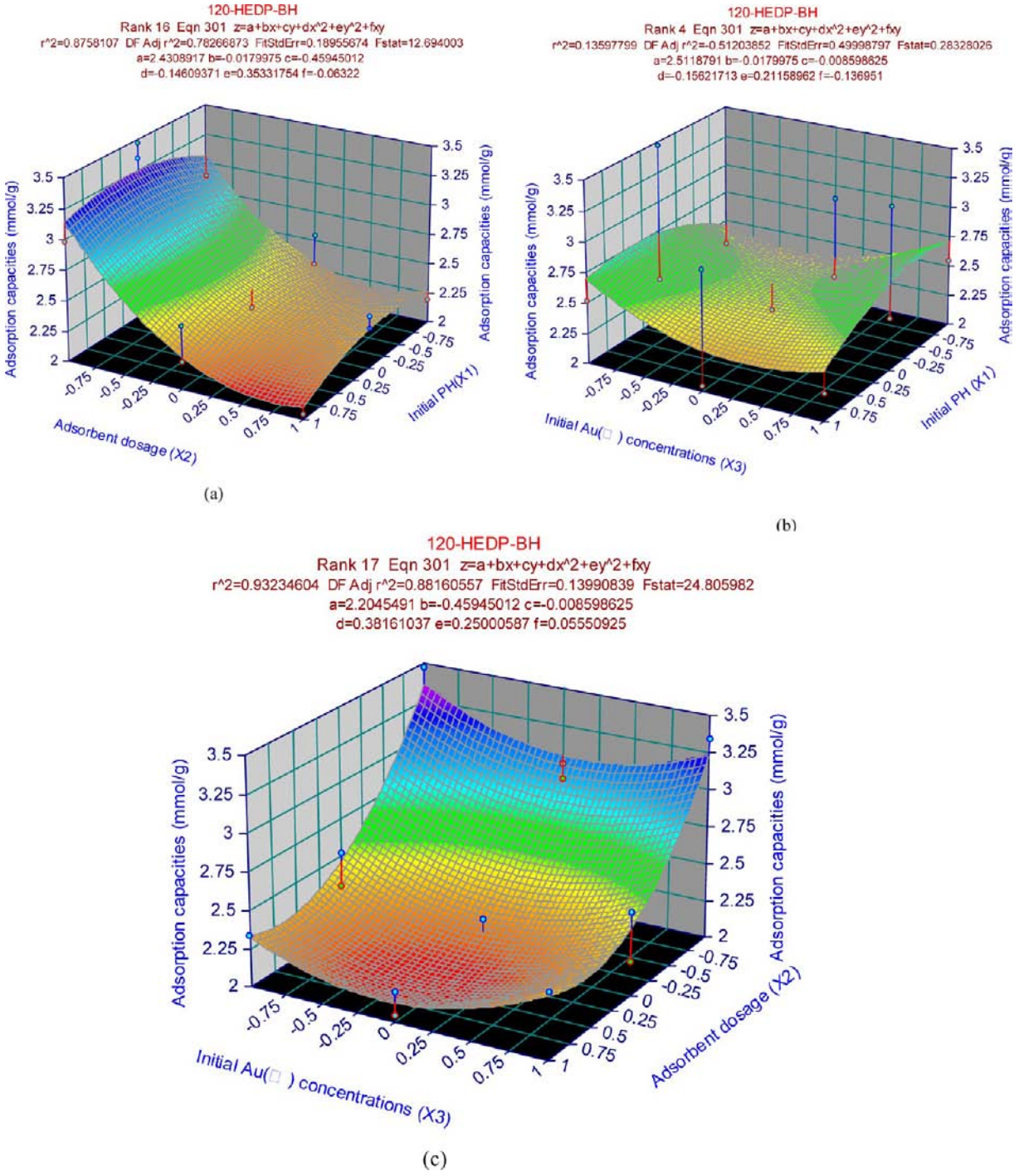

Figure 7. Interactions and response surfaces of the process variables on the adsorption capacities for Au(III) onto 120-HEDP-BH.

variation of 99.14% for the adsorption process was attributed to the independent variables and only 0.86% of the total variations was not explained by the model, and a higher value of the correction coefficient (R = 0.9957) justified an excellent correlation between the independent variables. Moreover, the insignificant lack-of-fit test also indicated that the model was suitable to represent the experimental data using the designed experimental data. [28]

The adsorption capacities of the adsorbent 120-HEDP-BH over different combinations of independent variables were visualized through three-dimensional view of response surface plots (Figure 7a–c). The relationship between adsorbent dosage and initial pH is shown in Figure 7a. Clearly, the adsorbent dosage exerted a stronger influence than initial pH, which could also be deduced from the coefficients of factors in eq 5. It was observed that the Au(III) adsorption capacities decreased with increasing 120-HEDP-BH dosage, though increasing adsorbent dosage can be attributed to increased biomass surface area and availability of more adsorption sites. Nevertheless, the values of Au(III) uptake decreased with increasing adsorbent dosage. The reason might be that high biomass dosage could result in aggregates of functionalized adsorbent 120-HEDP-BH and might cause interference between binding sites at higher biomass dosage or insufficiency

of metal ions in solutions with respect to available binding sites. The interaction between adsorbent dosage and initial pH was more insignificant (P = 0.118, and the absolute value of t value is −1.888). Furthermore, the initial pH also played an important role in gold ion uptake as evident from the equation and plot, and the effect of initial Au(III) concentrations and initial pH on gold uptake is shown in Figure 7b. The curved contour lines showed that there was an interaction between initial Au(III) concentrations and initial pH. A relatively strong interaction existed between initial Au(III) concentration and initial pH, which was reflected by the corresponding P value and deduced from the curvature of the contour. The research results showed that the gold adsorption capacity increased at first and then decreased with increasing pH, and the optimum pH was about 2.9. This may be explained by the increase in availability of binding sites at higher initial solution pH, and this improved in the access of gold ions to the metal-binding sites of the cell wall. The interaction between initial Au(III) concentrations and initial pH was very significant (P = 0.009, and the absolute value of t value is −4.089) and found to be responsible for achieving a relatively high gold ion uptake as predicted by the model and the response contour plot. Moreover, a moderate interaction was found between initial Au(III) concentration and adsorbent dosage (P = 0.158, and the absolute value of t value is 1.657), as shown in Figure 7c. According to the figure, at lower adsorbent dosage level, the Au(III) uptake efficiency increased slightly with increasing metal concentration from zero level up to a certain level; it could be due to the increase in the driving force of the concentration gradient. [9]

It is of general interest for developing an industrial process of gold adsorption from wastewater. On the basis of the discussion above, it was possible to obtain a high degree of adsorption capacity through searching for the optimum point. The maximum predicted adsorption capacity for optimum adsorption variables was obtained through the point prediction method and response surface plots. The optimal conditions for gold adsorption using the biomass-based adsorbent 120-HEDP-BH were an initial pH of 2.86, an initial Au(III) concentration of 6.07 and 10.0 mg/10.0 mL of adsorbent dosage, and a theoretical maximum adsorption capacity of 3.48 mmol/g. To confirm the prediction by the model, three independent experiments for the gold biosorption over 120-HEDP-BH were conducted under the established optimal conditions. The experimental adsorption capacity reached 3.30 ± 0.01 mmol/g and was close to the predicted value.

Adsorption Selectivity of 120-HEDP-BH. The most important properties of a chelating adsorbent material that influence its application are sorption amount in addition to sorption selectivity, which is basically an attribute of the functional group of the adsorbent. Therefore, the competitive adsorption experiments by 120-HEDP-BH were carried out for Au(III)−Hg(II), Au(III)−Ni(II), Au(III)−Cu(II), A (III)−Zn(II), Au(III)−Cd (II), and Au(III)−Co(II) binary systems. The initial Au(III) concentration as well as other transition metal ions such as Zn(II), Ni(II), and Cu(II) was 2.0 mmol/L, and the obtained results at 25 °C are presented in Table 6.

The selective coefficients were the ratio of adsorption amounts of metal ions in the binary mixture: The selective coefficient = q'/q'', where q' is the adsorption amount of Au(III) ion in a binary mixture and q'' is the adsorption amount of the other metal ion in binary mixture. Investigation on the adsorption selectivity showed that 120-HEDP-BH displayed

Table 6. Adsorption Selectivity of 120-HEDP-BH for Au(III)

adsorbent	system	metal ions	adsorbents capacity (mmol/g)	selective coefficient
120-HEDP-BH	Au(III)−Hg(II)	Au(III)	1.47	$\alpha_{Au(III)/Hg(II)}$ = 73.5
		Hg(II)	0.02	
	Au(III)−Ni(II)	Au(III)	1.46	$\alpha_{Au(III)/Ni(II)}$ = 146
		Ni(II)	0.01	
	Au(III)−Cu(II)	Au(III)	1.47	$\alpha_{Au(III)/Cu(II)}$ = 49.0
		Cu(II)	0.03	
	Au(III)−Zn(II)	Au(III)	1.48	$\alpha_{Au(III)/Zn(II)}$ = ∞
		Zn(II)	0.00	
	Au(III)−Cd(II)	Au(III)	1.47	$\alpha_{Au(III)/Cd(II)}$ = 24.5
		Cd(II)	0.06	
	Au(III)−Co(II)	Au(III)	1.48	$\alpha_{Au(III)/Co(II)}$ = ∞
		Co(II)	0.00	

strong affinity for gold in binary ions systems, and it even exhibited 100% selectivity for Au(III) ions in the presence of Zn(II) and Co(II). The adsorption experiments of Au(III) onto 120-HEDP-BH were carried out at pH 2.5, and the interactions of Au(III) ions with surface molecules of 120-HEDP-BH were dominated by adsorption, electrostatic attraction, and chelation (Figure S2, Supporting Information). The band at 2845 cm^{-1} assigned to the (P)−O−H stretching vibration before adsorption was obviously weakened after adsorption (see the IR spectrum of 120-HEDP-BH-Au in Figure 3), indicating the coordination of the phosphonic acid with gold(III) on 120-HEDP-BH. However, at lower pH, the functional groups of 120-HEDP-BH might remain primarily in the protonated form, making the adsorbent difficult for other heavy metal ions adsorption (such as Zn(II) etc.) to occur. Therefore, this novel 1-hydroxylethylidenediphosphonic acid-functionalized buckwheat hulls 120-HEDP-BH had a high adsorption amount and good selectivity for Au (III), which can be applied for removing this precious metal element from aqueous solutions.

Recycling Properties of 120-HEDP-BH. To investigate the feasibility of reusing the adsorbents 120-HEDP-BH, desorption experiments were conducted. The Au(III) ion loaded 120-HEDP-BH samples were treated with 0.1 mol/L hydrochloric acid and different concentrations of thiourea at 25 °C for 24 h to remove the Au(III) ions and then neutralized and followed with a second round of metal ion adsorption testing. The results of elution from Figure 8 show that the system of 3.0% thiourea + 0.1 mol/L HCl is very efficient, and the elution rate is up to 99.52%. The results for Au(III) ion adsorption using the regenerated adsorbents are summarized in Table 4. Only a little decrease of the adsorption efficiency was seen in the second use, the samples retain their Au(III) uptake capacities of 93.24% after two cycles, and the Au(III) uptake capacities decreased gradually in the successive uses. Therefore, the high adsorption capacity and good reproducibility gives the biomass-based adsorbent 120-HEDP-BH significant potential for removing Au(III) from aqueous solutions using the adsorption method.

Spent buckwheat hull is a kind of agriculture residue; it is a nontoxic and biodegradable biomass. 1-Hydroxylethylidenedi-

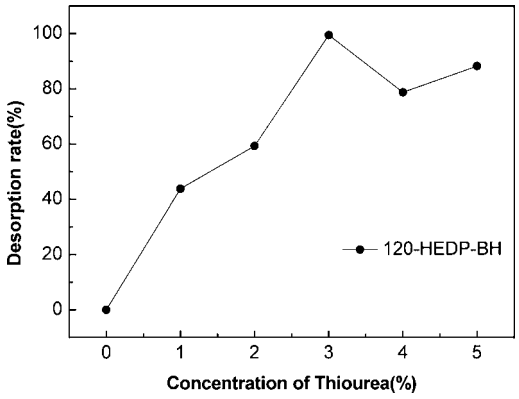

Figure 8. Effects of different concentrations of thiourea on the desorption rate.

Table 7. Regeneration Properties of 120-HEDP-BH

regeneration times		120-HEDP-BH
1	q (mmol/g)	0.94
	desorption rate(%)	99.52
2	q (mmol/g)	1.02
	desorption rate (%)	95.49
3	q (mmol/g)	0.96
	desorption rate (%)	93.24

phosphonic acid-functionalized buckwheat hulls (HEDP-BH) were successfully employed to adsorb heavy metal ions from stimulated wastewater. This study demonstrated that agricultural residues buckwheat hulls functionalized by organophosphonic acid could be a potential adsorbent for removing heavy metal ions from aqueous solutions, especially for Au(III) uptake. The maximum binding capacity of 120-HEDP-BH for Au(III) according to the Langmuir isotherm is 450.45 mg/g at 35 °C. From a practical point of view, the high adsorption capacity and efficiency and good selectivity should make 120-HEDP-BH a potential adsorbent. Moreover, it is evident that response surface methodology can be used successfully to gain knowledge to explain the relative performance of the adsorbent 120-HEDP-BH for Au(III) adsorption. The optimum values for maximum adsorption capacity could be obtained using a Box-Behnken center-united design with a minimum of experimental work. Under the optimal conditions, the predicted value of the adsorption capacity for Au(III) was 3.48 mmol/g. Therefore, the high adsorption capacity, good adsorption selectivity, and reproducibility give the biomass-based adsorbent 120-HEDP-BH significant potential for uptaking Au(III) from aqueous solutions using the adsorption method.

■ ASSOCIATED CONTENT

Supporting Information

The Supporting Information includes the effect of pH on Au(III) adsorption onto 120-HEDP-BH, the schematic diagram of Au(III) ions adsorption, the selected geometrical parameters and Mulliken atomic charges of the modified organic group 1-hydroxylethylidenediphosphonic acid obtained at the B3LYP/6-31G(d) level, and the adsorption capacities of different adsorbents for gold ions. Tables S1−S3 and Figures S1 and S2. This material is available free of charge via the Internet at http://pubs.acs.org.

■ AUTHOR INFORMATION

Corresponding Author

*E-mail: yinping426@163.com (P.Y.); rongjunqu@sohu.com (R.Q.).

Notes

The authors declare no competing financial interest.

■ ACKNOWLEDGMENTS

The support provided by the National Natural Science Foundation of China (51102127 and 51073075), the Nature Science Foundation of Shandong Province (2009ZRB01463), and the Foundation of Innovation Team Building of Ludong University (08-CXB001) were greatly appreciated. We also thank the helps given by Ludong University Dawning HPC Center.

■ REFERENCES

(1) Uchimiya, M.; Wartelle, L. H.; Klasson, K. T.; Fortier, C. A.; Lima, I. M. Influence of pyrolysis temperature on biochar property and function as heavy metal sorbent in soil. *J. Agric. Food Chem.* **2011**, *59*, 2501−2510.

(2) Anirudhan, T. S.; Sreekumari, S. S. Adsorptive removal of heavy metal ions from industrial effluents using activated carbon derived from waste coconut buttons. *J. Environ. Sci.* **2011**, *23* (12), 1989−1998.

(3) Uchimiya, S. M.; Lima, I. M.; Klasson, K. T.; Chang, S.; Wartelle, L. H.; Rodgers, J. E., III Immobilization of Heavy Metal Ions (CuII, CdII, NiII, and PbII) by Broiler Litter-Derived Biochars in Water and Soil. *J. Agric. Food Chem.* **2010**, *58* (9), 5538−5544.

(4) Cao, J.; Tan, Y.; Che, Y.; Xin, H. Novel complex gel beads composed of hydrolyzed polyacrylamide and chitosan: An effective adsorbent for the removal of heavy metal from aqueous solution. *Bioresour. Technol.* **2010**, *101*, 2558−2561.

(5) Bulgariu, D.; Bulgariu, L. Equilibrium and kinetics studies of heavy metal ions biosorption on green algae waste biomass. *Bioresour. Technol.* **2012**, *103*, 489−493.

(6) Altun, T.; Pehlivan, E. Removal of Cr(VI) from aqueous solutions by modified walnut shells. *Food Chem.* **2012**, *132*, 693−700.

(7) Lu, S.; Gibb, S. W. Copper removal from wastewater using spent-grain as biosorbent. *Bioresour. Technol.* **2008**, *99*, 1509−1517.

(8) Wu, Z.; Cheng, Z.; Ma, W. Adsorption of Pb(II) from glucose on thiol-functionalized cellulosic biomass. *Bioresour. Technol.* **2012**, *104*, 807−809.

(9) Ghorbani, F.; Younesi, H.; Ghasempouri, S. M.; Zinatizadeh, A. A.; Amini, M.; Daneshi, A. Application of response surface methodology for optimization of cadmium biosorption in an aqueous solution by Saccharomyces cerevisiae. *J. Chem. Eng.* **2008**, *145*, 267−275.

(10) Ding, D. G.; Yin, M. C.; Lu, H. J.; Fan, Y. T.; Hou, H. W.; Wang, Y. T. A novel copper diphosphonate complex Cu4(aedp)2(4,4′-bipy)(H2O)4 with three-dimensional framework structure. *J. Solid State Chem.* **2006**, *179*, 747−752.

(11) Latham, K.; White, K. F.; Szpakolski, K. B.; Rix, C. J.; White, J. M. Synthesis, crystal structure and luminescent behaviour of coordination complexes of copper with bi- and tridentate amines and phosphonic acid. *Inorg. Chim. Acta* **2009**, *362*, 1872−1886.

(12) Joswig, J. O.; Hazebroucq, S.; Seifert, G. Properties of the phosphonic-acid molecule and the proton transfer in the phosphonic-acid dimer. *J. Mol. Struc: THEOCHEM* **2007**, *816*, 119−123.

(13) Qu, R.; Wang, M.; Sun, C.; Zhang, Y.; Ji, C.; Chen, H.; Meng, Y.; Yin, P. Chemical modification of silica-gel with hydroxyl- or amino-terminated polyamine for adsorption of Au(III). *Appl. Surf. Sci.* **2008**, *255*, 3361−3370.

(14) Yu, M.; Sun, D.; Tian, W.; Wang, G.; Shen, W.; Xu, N. Systematic studies on adsorption of trace elements Pt, Pd, Au, Se, Te, As, Hg, Sb on thiol cotton fiber. *Anal. Chim. Acta* **2002**, *456*, 147−155.

(15) Gamez, G.; Gardea-Torresdey, J. L.; Tiemann, K. J.; Parsons, J.; Dokken, K.; Yacaman, M. J. Recovery of gold (III) from multi-

elemental solutions by alfalfa biomass. *Adv. Environ. Res.* **2003**, *7*, 563−571.
(16) Jermakowicz-Bartkowiak, D.; Kolarz, B. N.; Serwin, A. Sorption of precious metals from acid solutions by functionalised vinylbenzyl chloride-acrylonitryle-divinylbenzene copolymers bearing amino and guanidine ligands. *React. Funct. Polym.* **2005**, *65*, 135−142.
(17) Chen, H.; Li, J.; Shen, T.; Li, Y.; Liu, J.; Liu, J.; Xu, A.; Wang, C. Gold(III) tetraarylporphyrin phosphonate derivatives as potential anticancer agents. *J. Chem. Res.* **2012**, *36*, 501−505.
(18) Kojima, M.; Mikami, K. Enantioselective Intramolecular Hydroamination of *N*-Alkenyl Ureas Catalyzed by *tropos* BIPHEP-Gold(I) Complexes with Au-Au Interaction. *Synlett* **2012**, *2012* (1), 57−61.
(19) Gardea-Torresdey, J. L.; Tiemann, K. J.; Parsons, J. G.; Gamez, G.; Jose Yacaman, M. Characterization of trace level Au(III) binding to alfalfa biomass (Medicago sativa) by GFAA. *Adv. Environ. Res.* **2002**, *6*, 313−323.
(20) Yin, P.; Wang, C.; Yang, Y.; Tian, Y.; Yu, Z. Thermodynamics and Kinetics of Au(III) Adsorption on Silica Gel Chemically Modified by Diethylenetriamine Bis(methylene phosphonic acid). *J. Chem. Eng. Data* **2011**, *56*, 450−457.
(21) Dobrowolski, R.; Kurylo, M.; Otto, M.; Mroz, A. Determination of gold in geological materials by carbon slurry sampling graphite furnace atomic absorption spectrometry. *Talanta* **2012**, *99*, 750−757.
(22) Zammit, C. M.; Cook, N.; Brugger, J.; Ciobanu, C. L.; Reith, F. The future of biotechnology for gold exploration and processing. *Miner. Eng.* **2012**, *32*, 45−53.
(23) Navarro, P.; Vargas, C.; Alonso, M.; Alguacil, F. J. Towards a more environmentally friendly process for gold: models on gold adsorption onto activated carbon from ammoniacal thiosulfate solutions. *Desalination* **2007**, *211*, 58−63.
(24) Tay, T.; Ucar, S.; Karagoz, S. Preparation and characterization of activated carbon from waste biomass. *J. Hazard. Mater.* **2009**, *165*, 481−485.
(25) Ho, Y. S. Selection of optimum sorption isotherm. *Carbon* **2004**, *42*, 2115−2116.
(26) Jing, X.; Cao, Y.; Zhang, X.; Wang, D.; Wu, X.; Xu, H. Biosorption of Cr(VI) from stimulated wastewater using a cationic surfactant modified spent mushroom. *Desalination* **2011**, *269*, 120−127.
(27) Khuri, A. I.; Cornell, J. A. *Response surface: design and analysis*; New York: Marcel Dekker, 1987.
(28) Yalvac can, M.; Kaya, Y.; Faruk Algur, O. Response surface optimization of the the removal of nickel from aqueous solution by cone biomass of Pinus sylvestris. *Bioresour. Technol.* **2006**, *97*, 1761−1765.